

AROMATICS GROWTH BEYOND THE FIRST RING AND THE NUCLEATION OF SOOT PARTICLES

Michael Frenklach and Hai Wang
Fuel Science Program
Department of Materials Science and Engineering
The Pennsylvania State University
University Park, PA 16802

Keywords: soot formation, reaction mechanism and chemical kinetics of, particle dynamics of

INTRODUCTION

In this manuscript, we discuss the the reaction mechanism responsible for the formation and growth of polycyclic aromatic hydrocarbons (PAHs) and subsequent nucleation and growth of soot particles in combustion of hydrocarbon fuels. The discussion is based on the results of a detailed chemical kinetic study,¹ and we refer the reader to this reference for the computational details. Here, we focus on the principal reaction pathways and mechanistic features identified in the analysis.

OVERALL PROCESS

The overall model of soot formation can be thought of as consisting of four major processes: *initial PAH formation*, which includes the formation of the first aromatic ring in an aliphatic system; *planar PAH growth*, comprised of replicating-type growth; *particle nucleation*, consisting of coalescence of PAHs into three-dimensional clusters; and *particle growth* by coagulation and surface reactions of the forming clusters and particles. Our primary attention in this discussion is on the last three processes, although some comments are pertinent concerning the formation of the first aromatic ring.

Formation of the First Aromatic Ring

The formation of the first aromatic ring in flames of nonaromatic fuels begins usually with vinyl addition to acetylene. At high temperatures, it forms vinylacetylene followed by acetylene addition to *n*-C₄H₃ radical formed by the H-abstraction from the vinylacetylene (Fig. 1). At low temperatures, the addition of acetylene to vinyl results in *n*-C₄H₅, which upon addition of acetylene produces benzene. Benzene and phenyl are converted to one another by the H-abstraction reaction and its reverse.

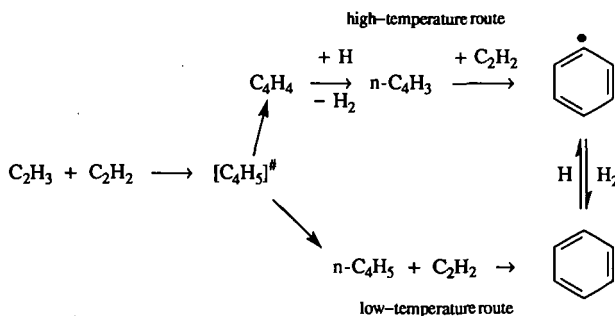


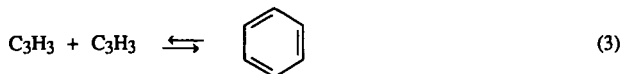
Figure 1. Formation of the first aromatic ring

In a recent review article on chemical kinetics and combustion modeling, Miller, Kee and Westbrook² suggested that the above cyclization reactions cannot be responsible for the formation of the first aromatic ring because the concentrations of *n*-C₄H₃ and *n*-C₄H₅ radicals should be low since the reactions



deplete the concentrations of the *n*-isomers required for the cyclizations. Reactions (1) and (2) were not included in our model. Our computational results indicated that the *n*- and *i*-isomers are already equilibrated by several other reactions in the system. Nonetheless, to test the Miller *et al.*'s suggestion, we performed additional simulations of the three laminar premixed flames we analyzed previously.^{1,3} The reactions (1) and (2) were now included in the simulations assuming rate coefficients $1 \times 10^{14} \text{ mol cm}^{-3} \text{ s}^{-1}$ for the exothermic directions. The results of these simulations for all the three flames tested in Refs. 3 indicated that the inclusion of reactions (1) and (2) — even with upper-limit rate coefficient values — does not make a difference on the computed profile of benzene.

As an alternative, Miller *et al.*² suggested that benzene is formed by combination of propargyl radicals producing benzene or phenyl. A similar proposal was made by Stein *et al.*⁴ Figures 2 and 3 show the results of flame simulations with reaction



included with the rate coefficient of $5 \times 10^{12} \text{ mol cm}^{-3} \text{ s}^{-1}$ suggested by Stein *et al.*⁴ Analysis of these results indicate that the inclusion of cyclization channel (3) does not *always* increase the production rate of benzene, as clearly shown in Fig. 2 for the flame conditions of Harris and co-workers.⁵ For the conditions of the Westmoreland's flame,⁶ the inclusion of reaction (3) significantly overpredicts the amount of benzene determined experimentally (Fig. 3). This is clearly a challenging issue, as the reaction chemistry of C₃H_x species is not well known.

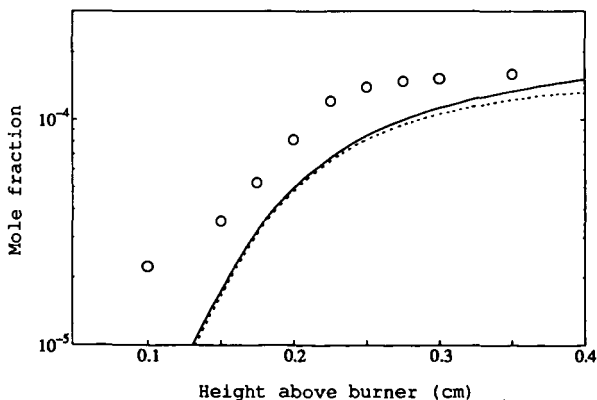


Figure 2. Benzene mole fraction: circles — experimental data,⁵ solid line — computed with the mechanism used in Refs. 1 and 3, dotted line — computed with reaction (3) included

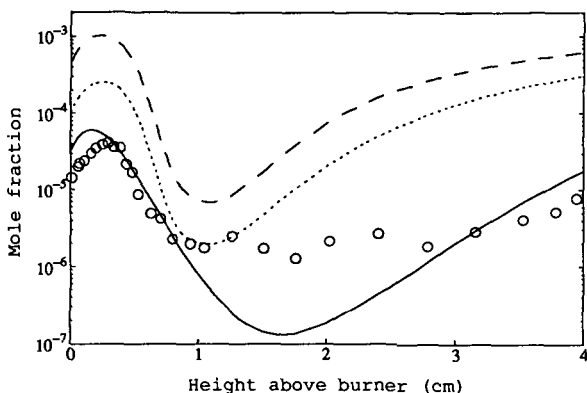


Figure 3. Benzene mole fraction: circles — experimental data;⁶ solid line — computed with the mechanism used in Refs. 1 and 3; dashed and dotted lines — computed with reaction (3) included, dotted line represents the result computed with the mechanism tuned to fit the experimental C_3H_3 profile

Growth of the Aromatic Rings

Once formed, aromatic rings grow by a sequential two-step process: H-abstraction which activates the aromatic molecules, and acetylene addition which propagates molecular growth and cyclization of PAHs (Fig. 4).

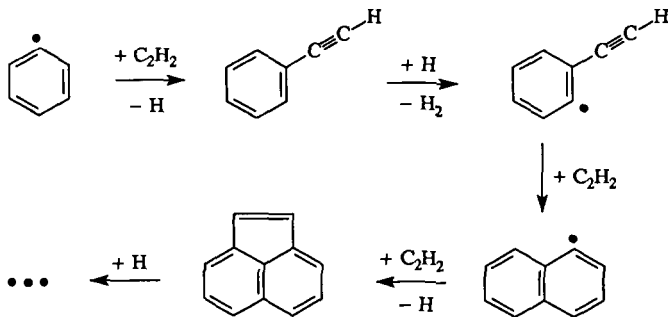


Figure 4. H-abstraction- C_2H_2 -addition reaction pathway of PAH growth

Starting with an aromatic fuel, a "direct" condensation of intact aromatic rings becomes important. For example, in the case of high-temperature pyrolysis of benzene the reactions shown in Fig. 5 were found to dominate the initial stages of PAH growth.⁷

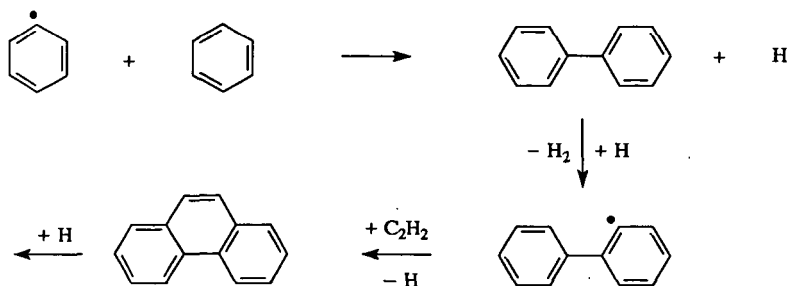
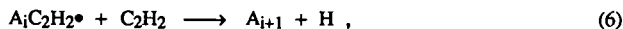


Figure 5. PAH growth initiated by aromatics "condensation"

However, as the reaction progresses, the initial benzene molecules decompose, primarily forming acetylene. As the concentration of acetylene approaches that of benzene, which occurs shortly after the initial period, the PAH growth switches to the acetylene-addition mechanism discussed above for nonaromatic fuels. In other words, the reaction system *relaxes* to the acetylene-addition pathway. The relaxation is faster in oxidation⁸ as compared to pyrolysis and in mixtures of hydrocarbons⁹ as compared to individual fuels.

Some of the acetylene addition reactions in the PAH growth sequence form particularly stable aromatic molecules, like pyrene, coronene, etc. The change of the free energy in these reactions is so large that the reactions become practically irreversible. This, in turn, has an effect of "pulling" the reaction sequence forward, towards formation of larger PAH molecules. Other acetylene addition steps are highly reversible, i.e., the rate of the forward reaction is nearly balanced by the rate of the reverse reaction. These steps with tightly balanced reaction fluxes create a thermodynamic barrier to PAH growth. It is this thermodynamic "resistance" which is responsible for the appearance of most stable, condensed aromatic structures, as opposite to open shell carbon clusters leading to fullerenes.¹⁰ For instance, due to small differences in reaction enthalpies, the reaction flux from phenanthrene to benzo[ghi]perylene shown on the left of Fig. 6 was computed¹¹ to be faster by an order of magnitude than the one on the right hand side of Fig. 6.

The main kinetic features of PAH growth after a certain PAH size, i_0 , can be schematically represented by the following set of reactions¹²



where A_i denotes an aromatic molecule containing i fused aromatic rings ($i = i_0, i_0+1, \dots, \infty$), A_i^\bullet is an aromatic radical formed by the abstraction of an H atom from A_i , and $A_iC_2H_2^\bullet$ is a radical formed by the addition of C_2H_2 to A_i^\bullet . It is assumed that reactions (5) and (6) are reversible and reaction step (6) is irreversible. The rate of PAH mass accumulation is proportional to

$$\text{Rate} = \frac{K_4 \frac{[H]}{[H_2]}}{\frac{1}{K_5 k_6 [C_2H_2]^2} + \frac{1}{k_5 [C_2H_2]} + \frac{1}{k_{-4} [H_2]}} \int r_0 dt, \quad (7)$$

where t is the reaction time, r_0 is the rate of irreversible formation of A_{i0} by initiation reactions, k_j is the rate coefficient of the j th reaction, and $K_j = k_j/k_{-j}$ is the equilibrium constant of the j th reaction.

In this equation, term $\int r_0 dt$ represents the contribution of the initiation reactions, i.e., those leading to the formation of first few PAHs. Term $K_4 \frac{[H]}{[H_2]}$ accounts for the "equilibrium position" or, in more rigorous terms, reaction affinity of reaction (1); it represents the superequilibrium of H atoms — the first kinetic factor responsible for PAH growth. Term $k_6[C_2H_2]$ is the effective rate constant of the irreversible addition of acetylene, reaction (6), forming particular stable PAH molecules — the second kinetic factor responsible for PAH growth. Terms $k_5[C_2H_2]$ and $K_5[C_2H_2]$ specify kinetic and thermodynamic factors, respectively, of the reversible addition of acetylene, reaction (5); the latter expresses the thermodynamic resistance to PAH growth. And finally, term $k_{-4}[H_2]$ accounts for the effective rate constant of the H-abstraction, reaction (4); to illustrate it, consider the limit of $k_{-4}[H_2] \rightarrow 0$ under which condition the ratio in Eq. (7) reduces to $k_4[H]$. At high pressures, reaction



should contribute to the overall balance of the A_i^\bullet radical, and at a high concentration of hydrogen atoms, such that $k_8[H] \gg k_{-4}[H_2]$, we obtain an interesting limit of the PAH growth rate being independent of the H concentration.

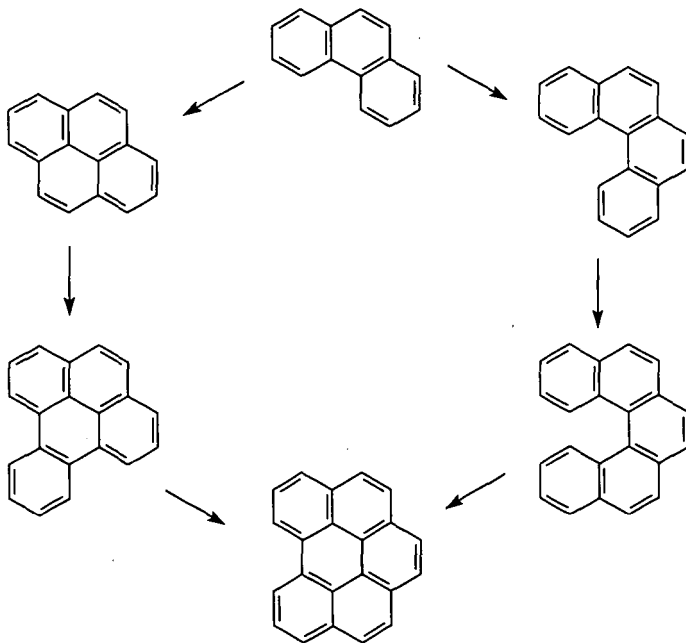


Figure 6. Comparison of two pathways of PAH growth.

An additional kinetic factor, $k_9[\text{O}_2]$, where k_9 is the rate coefficient of oxidation reaction

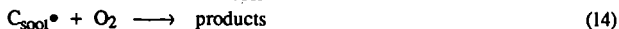
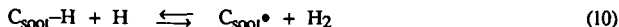


is introduced in oxidative environments. Although many oxidative reaction channels are possible, it appeared, as a result of our kinetic analysis of shock-tube oxidation⁸ and flame¹³ environments, that PAH removal by oxidation occurs predominantly via molecular oxygen attack on aromatic radicals. Also, due to similar reactions of O_2 with C_2H_3 and C_4H_3 radicals (and of OH with C_2H_2 , *etc.*), the concentrations of these critical intermediates are decreased, which in turn reduces the formation rate of the first aromatic ring. At the same time, the presence of O_2 in the mixture has a promoting effect on aromatics formation because of the accelerated chain branching leading to enhanced fuel pyrolysis and thus increased production of critical intermediates and hydrogen atoms. The balance of all of these factors determines the net effect of oxygen addition.

Nucleation and Growth of Soot Particles

We have developed a detailed kinetic model of soot particle formation and growth in the following manner. The formed PAH species were allowed to *coagulate*, that is, all the A_i 's ($i = 4, 5, \dots, \infty$) collide with each other forming dimers; the dimers, in turn, collide with A_i forming trimers or with other dimers forming tetramers; and so on. The coalescence reactions were treated as irreversible having sticking coefficients of unity. As the focus of this work is on very young, small particles, it was assumed that the coagulation dynamics is in the free-molecular regime.

Beginning with the dimers, the forming clusters were assumed to be "solid phase" and allowed to add and lose mass by surface reactions



where $\text{C}_{\text{soot}}\text{-H}$ represents an arm-chair site on the soot particle surface and $\text{C}_{\text{soot}}^\bullet$ the corresponding radical. This mechanism is adopted based on the postulate^{1,14} that the H-abstraction/ C_2H_2 -addition reaction sequence above is responsible for high-temperature growth of all forms of carbonaceous materials. Following this postulate, the rate coefficients of the heterogeneous reactions (10)–(15) were estimated based on analogous gas-phase reactions of one-ring aromatics, benzene and phenyl. In doing so, it was assumed that collision efficiencies on a per-site basis are the same for both gas-phase and gas-solid reactions. The particle dynamics — the evolution of soot particles undergoing simultaneous nucleation, coagulation and surface reactions described above — was modeled by a method of moments which does not require the assumption of a particle size distribution function.

The model predictions were found¹ in relatively close agreement with experiment for such properties as soot particle number density, specific surface area, average soot particle diameter, and laser-light scattering moments for the initial, particle inception part of several simulated laminar premixed flames. The reliability of the model was further supported by the facts that the computed net surface growth rate is in close agreement with that determined by Harris and Weiner¹⁵ and that the predicted rate of soot oxidation by O_2 agrees well with the expression of Nagle and Strickland-Constable.¹⁶

Some major results of this modeling study¹ are summarized below:

- (i) The computed rate of nucleation is balanced by the rate of coagulation throughout the particle inception zone, however, the nucleation rate decays more slowly with flame height than is usually deduced from experiment;
- (ii) Particle inception is primarily determined by PAH coagulation, initiated and controlled by PAH coalescence into dimers. For instance, excluding all surface processes results in a substantial decrease of the particle mass but does not really change the order of magnitude of the particle size. In other words, the particle size is essentially determined by coagulation;
- (iii) While the average soot particle is computed to contain 10^3 – 10^5 carbon atoms, the corresponding average PAH size is only 20 to 50 carbon atoms. This indicates that the crystallites comprising incipient soot particles should be on the order of 7 to 12 Å, in agreement with experiment¹⁷ and against the proposal that soot is formed via spheroidal, polyhedral carbon clusters;
- (iv) The oxidation by OH and O₂ is quite insignificant in the post-flame zone;
- (v) The surface growth of soot mass is primarily determined by two processes: acetylene addition via the H-abstraction/C₂H₂-addition reaction sequence, and PAH condensation on the particle surface. The relative contribution of each of these processes appears to change with experimental conditions. Thus, while the acetylene addition dominates surface growth in an atmospheric ethylene flame of Harris *et al.*,⁵ PAH condensation prevails in a low-pressure acetylene flame of Bockhorn and co-workers.¹⁸ The main contribution of the PAH condensation occurs at the early stages of PAH coagulation;
- (vi) The model predicts the classical structure of soot particles: a less dense particle core, composed of randomly oriented PAH oligomers, and a more dense concentrically-arranged particle shell;
- (vii) Surface processes can be understood in terms of elementary chemical reactions of surface active sites. The number density of these sites is determined by the chemical environment.

ACKNOWLEDGEMENTS

The computations were performed using the facilities of the Pennsylvania State University Center for Academic Computing. Research was sponsored by the Air Force Office of Scientific Research, Air Force Systems Command, USAF, under grant No 88-0072. The US Government is authorized to reproduce and distribute reprints for Governmental purposes notwithstanding any copyright notation thereon.

REFERENCES

1. Frenklach, M. and Wang, H., "Detailed Modeling of Soot Particle Formation and Growth," *Twenty-Third Symposium (International) on Combustion*, in press.
2. Miller, J. A., Kee, R. J. and Westbrook, C. K., *Annu. Rev. Phys. Chem.* 41, 345 (1990).
3. Wang, H. and Frenklach, M., "Modeling of PAH Profiles in Premixed Flames," Fall Technical Meeting of the Eastern States Section of the Combustion Institute, Albany, New York, October 1989.
4. Stein, S. E., Walker, J. A., Suryan, M. M., and Fahr, A., "A New Path to Benzene in Flames," *Twenty-Third Symposium (International) on Combustion*, in press.

5. Harris, S. J., Weiner, A. M., Blint, R. J., and Goldsmith, J. E. M., *Twenty-First Symposium (International) on Combustion*, The Combustion Institute, Pittsburgh, 1988, p.1033; Harris, S.J., Weiner, A.M., and Blint, R.J., *Combust. Flame* **72**, 91 (1988).
6. Westmoreland, P. R., "Experimental and Theoretical Analysis of the Oxidation and Growth Chemistry in a Fuel-Rich Acetylene Flame," Ph.D. thesis, MIT, 1986.
7. Frenklach, M., Clary, D. W., Gardiner, W. C., Jr., and Stein, S. E., *Twenty-First Symposium (International) on Combustion*, The Combustion Institute, Pittsburgh, 1988, p. 1067.
8. Frenklach, M., Clary, D. W., Yuan, T., Gardiner, W. C., Jr., and Stein, S. E., *Combust. Sci. Technol.* **50**, 79 (1986).
9. Frenklach, M., Yuan, T., and Ramachandra, M. K., *Energy & Fuels* **2**, 462 (1988).
10. Frenklach, M. and Ebert, L.B., *J. Phys. Chem.* **92**, 561 (1988).
11. Frenklach, M., Clary, D.W., Gardiner, W.C., Jr., and Stein, S.E., *Twentieth Symposium (International) on Combustion*, The Combustion Institute, 1985, p. 887.
12. Frenklach, M., *Twenty-Second Symposium (International) on Combustion*, The Combustion Institute, Pittsburgh, 1989, p. 1075.
13. Frenklach, M. and Warnatz, J., *Combust. Sci. Technol.* **51**, 265 (1987).
14. Frenklach, M., "A Unifying Picture of Gas-Phase Formation and Growth of PAH, Soot, Diamond and Graphite," in *Carbon in the Galaxy: Studies from Earth and Space*, J. Tarter, S. Chang, and D. J. DeFrees, Eds., NASA CP 3061, 1990, p. 259.
15. Harris, S.J. and Weiner, A.M., *Combust. Sci. Technol.* **32**, 267 (1983).
16. Nagle, J. and Strickland-Constable, R.F., *Proceedings of the Fifth Conference on Carbon*, Pergamon, London, 1962, p. 154.
17. Ebert, L.B., Scanlon, J.C. and Clausen, C.A., *Energy & Fuels* **2**, 438 (1988).
18. Wieschnowsky, U., Bockhom, H. and Fetting, F., *Twenty-Second Symposium (International) on Combustion*, The Combustion Institute, 1989, p. 343.